BIOSYSFOODENG 2025 – THE INTERNATIONAL CONFERENCE ON BIOSYSTEM AND FOOD ENGINEERING IN BUDAPEST, HUNGARY

SYNTHESIS OF Fe_3O_4/GRAPHENE OXIDE NANOCOMPOSITES ON SUGARCANE BAGASSE-DERIVED ACTIVATED CARBON FOR Cr(VI) REMOVAL FROM AQUEOUS SOLUTIONS

Bi Duy Tran, Van Thanh Thi Le

Department of Chemical Engineering, Faculty of Chemical Engineering and Food Technology, Nong Lam University, Ho Chi Minh City, Vietnam.

Email: thvan@hcmuaf.edu.vn

Introduction

The rapid advancement of agriculture and industry has inadvertently contributed to water pollution, with Cr(VI) emerging as a critical concern due to its high toxicity, posing severe health risks such as kidney failure, liver disease, and lung cancer.

Adsorption is widely used for water treatment, thus driving the search for efficient, cost-effective, and eco-friendly adsorbents. In this context, sugarcane bagasse-derived activated carbon (AC) offers a large surface area, reduces agricultural waste, and promotes sustainable environmental solutions.

Graphene oxide (GO) is easily functionalizable due to its oxygen-rich composition and large surface area. Meanwhile, magnetite (Fe_3O_4) enables efficient magnetic separation due to its strong magnetic properties. However, high production costs remain a significant barrier to the application of GO and Fe_3O_4 in water treatment. Therefore, integrating AC, GO, Fe_3O_4 aims to reduce material costs, overcome individual limitations, and enhance Cr(VI) removal efficiency.

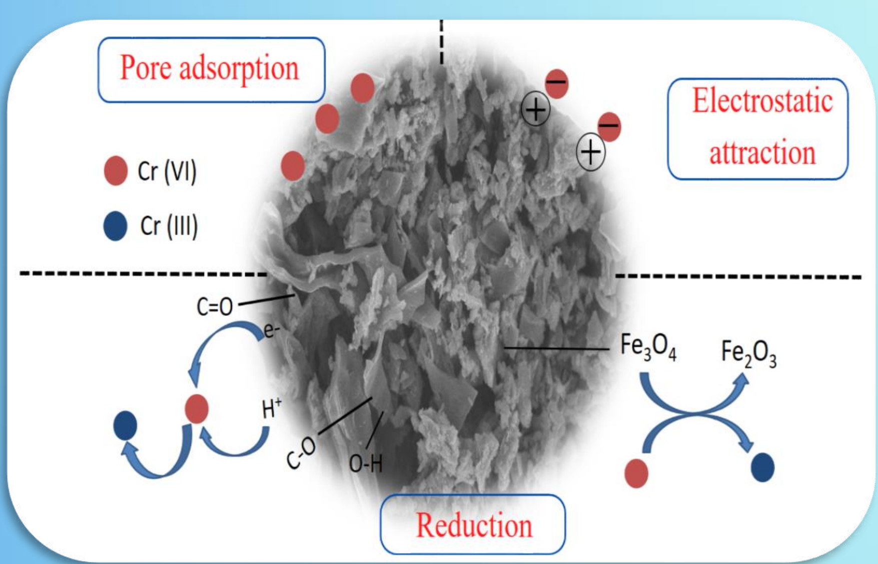

Fig 1. Possible schematic mechanism of Cr (VI) interaction with AC/GO/Fe_3O_4

Synthesis process

Fig 2. Synthesis process of activated carbon from sugarcane bagasse (AC)

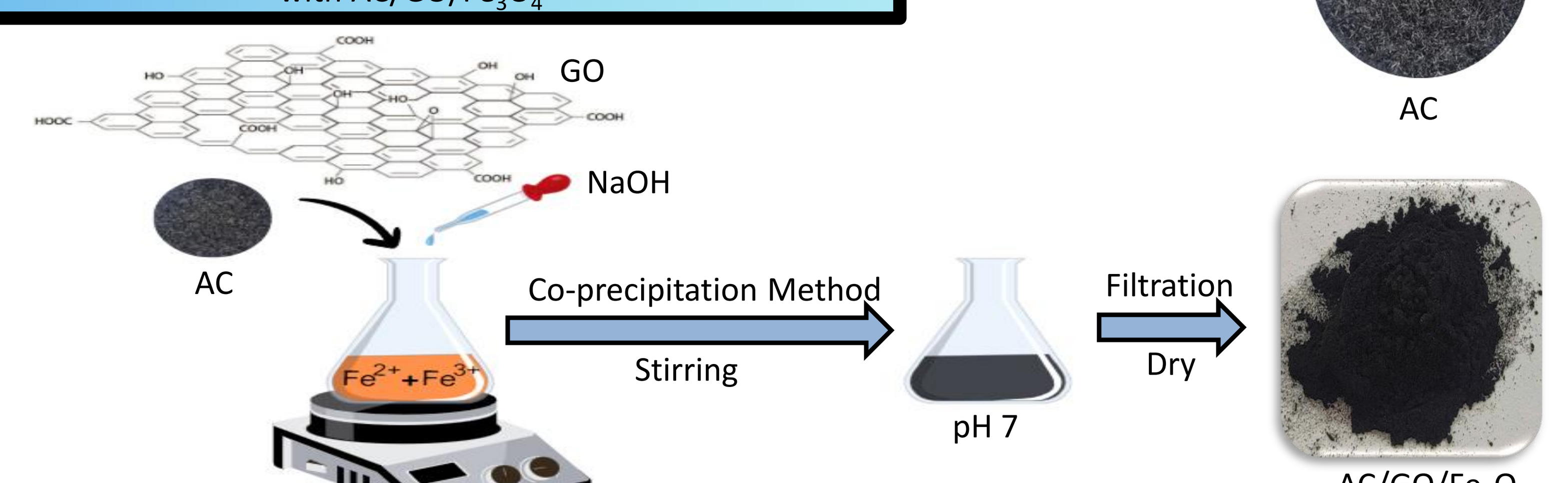

Fig 3. Synthesis process of AC/GO/Fe_3O_4

Characterization of AC/GO/Fe_3O_4

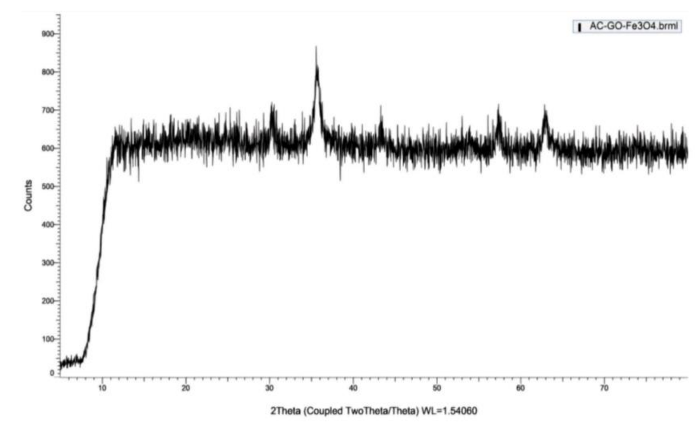

Fig 4. XRD analysis of AC/GO/Fe_3O_4

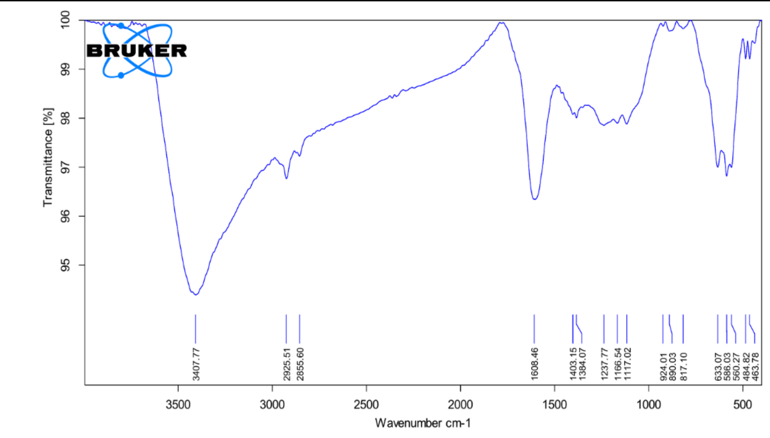

Fig 5. FTIR analysis of AC/GO/Fe_3O_4

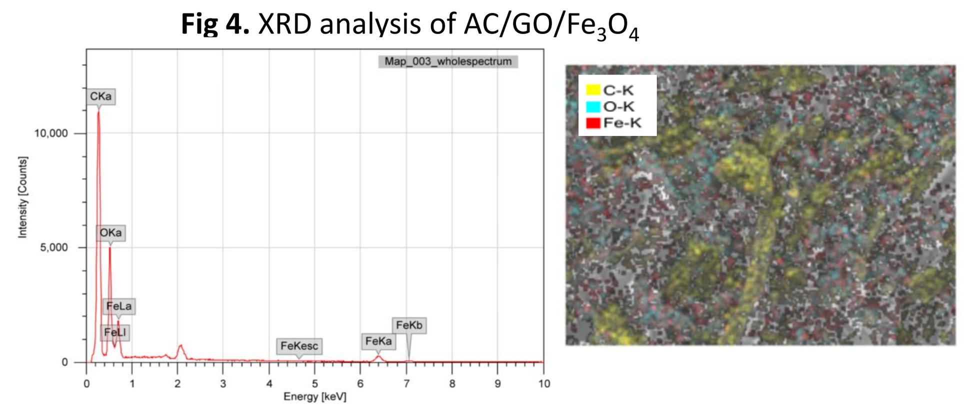

Fig 6. EDX spectrum of AC/GO/Fe_3O_4

Table 1. The composition of AC/GO/Fe_3O_4

Element	Mass (%)	Atom (%)
C	51,52±0,1	69,63±0,14
O	22,48±0,13	22,81±0,13
Fe	26,00±0,58	7,56±0,17

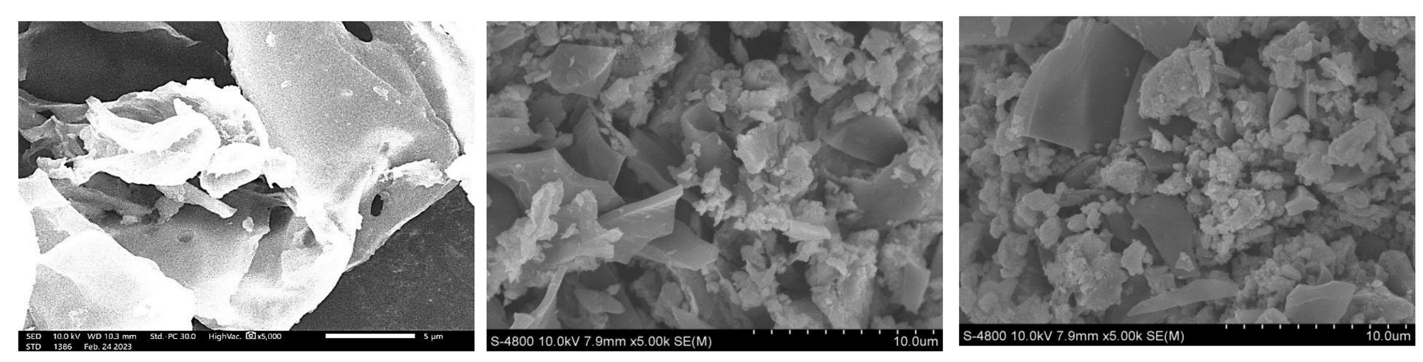

Fig 7. SEM image of AC (A), AC/GO/Fe_3O_4 before adsorption (B) and AC/GO/Fe_3O_4 after adsorption (C)

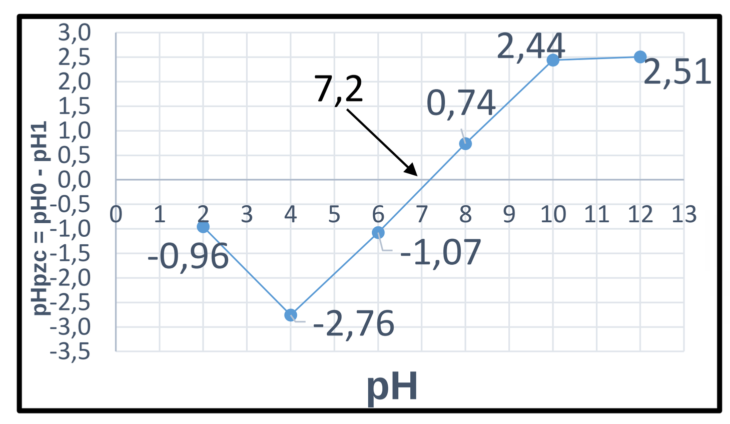

Fig 8. Point of zero charge (pHpzc)

$S_{BET\ AC}$ = 528,71 m^2/g

$S_{BET\ AC/GO/Fe3O4}$ = 312,47 m^2/g

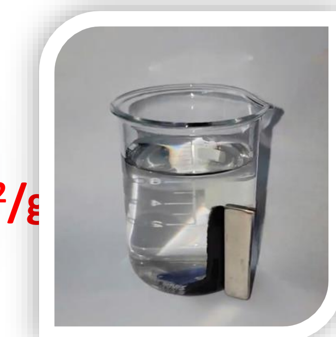

Fig 9. The magnetic of AC/GO/Fe_3O_4

The interaction effects of factors on Cr (VI) adsorption

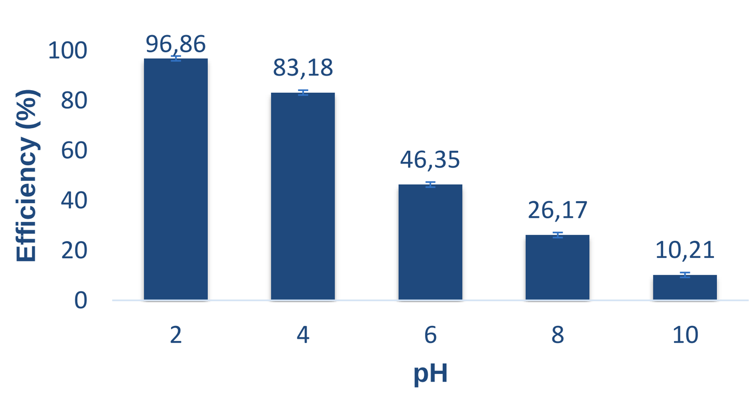

Fig 10. The effect of the pH

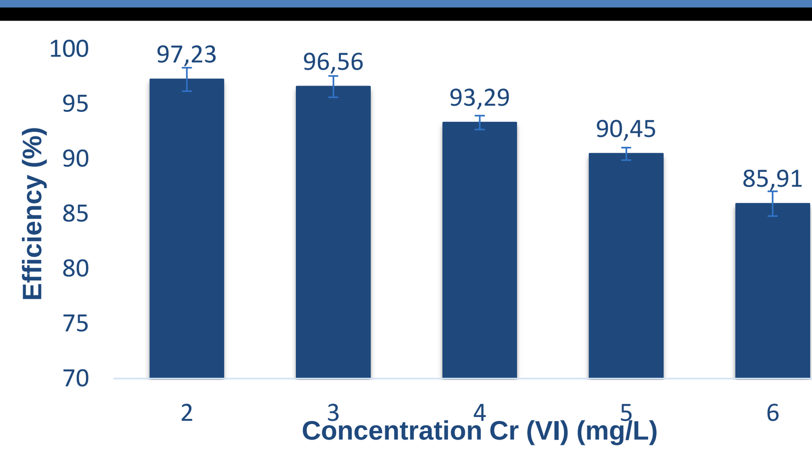

Fig 11. The effect of the concentration Cr (VI)

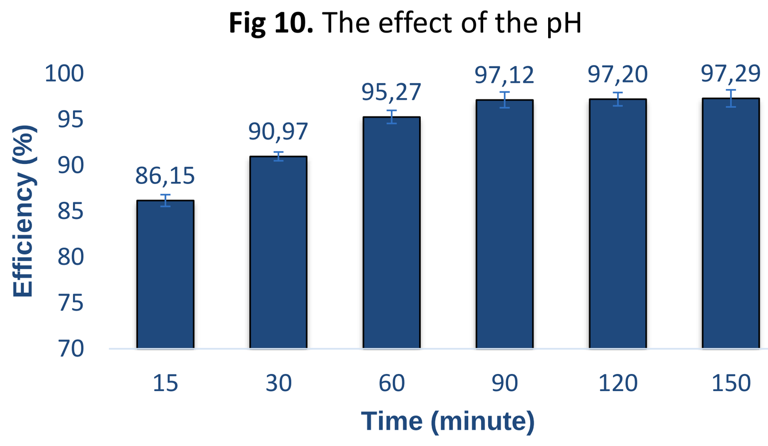

Fig 12. The effect of time

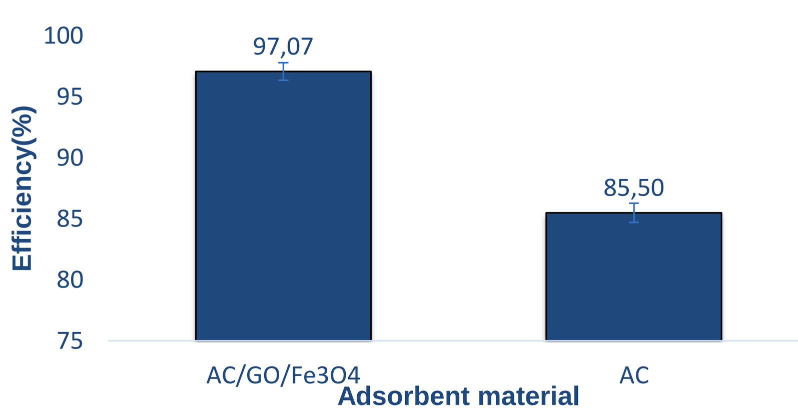

Fig 13. Comparison of Cr (VI) adsorption efficiency between AC/GO/Fe_3O_4 and AC

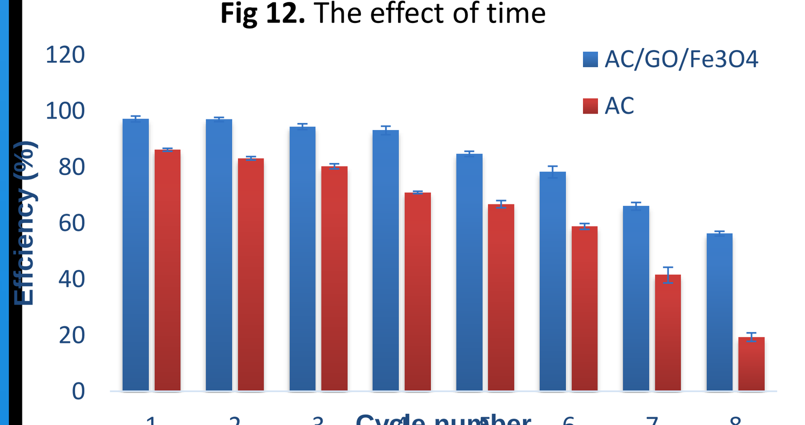

Fig 14. Adsorption efficiency of Cr (VI) over multiple adsorption – desorption cycles

Table 2. Several optimal conditions for Cr (VI) adsorption on AC/GO/Fe_3O_4

Influencing factors	Optimal conditions
pH	2
Concentration Cr (VI) (mg/L)	3
Mass of AC/GO/Fe_3O_4 (g)	0,04
Time (minute)	90
Efficiency (%)	≈ 97%

Adsorption isotherm and adsorption kinetics

Table 3. The Langmuir and Freundlich isotherms constants for Cr (VI) adsorption on AC/GO/Fe_3O_4.

Langmuir				Freundlich			
Q_m (mg/g)	K_L	R_L	R^2	1/n	n	K_F	R^2
14,27	8,30	0,06÷0,02	0,99	0,34	2,94	14,33	0,96

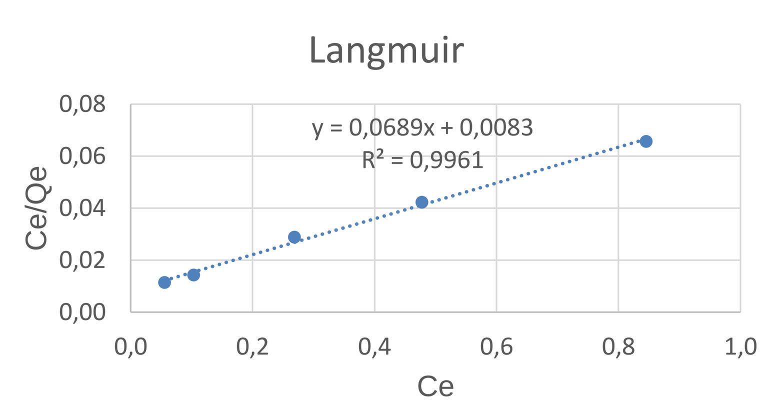

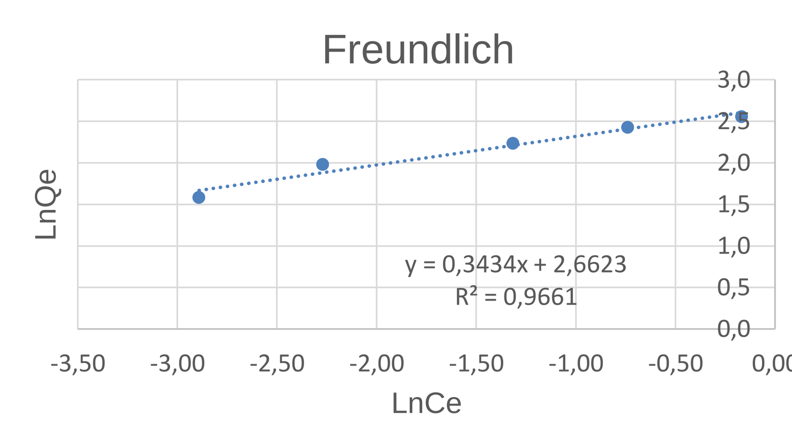

Table 4. The kinetic models parameters for Cr (VI) adsorption on AC/GO/Fe_3O_4.

Pseudo-first-order			Pseudo-second-order			Experimental
q_e (mg/g)	K_1 ($minute^{-1}$)	R^2	q_e (mg/g)	K_2 (g/mg.minute)	R^2	q_e
0,68	0,0496	0,97	7,42	0,06	1	7,28

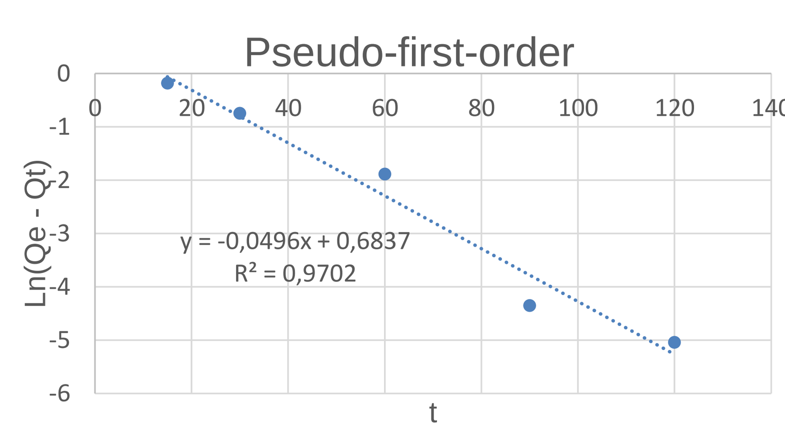

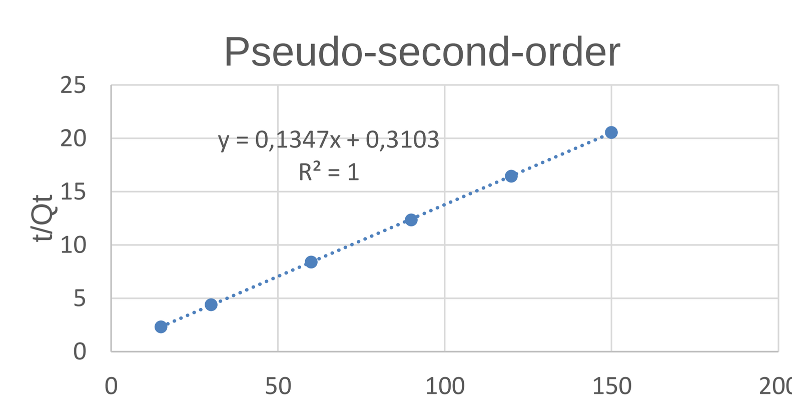

Conclusion

In this study, AC/GO/Fe_3O_4 was successfully synthesized via the co-precipitation method, with AC accounting for 50% of the total mass. BET analysis revealed a specific surface area (S_{BET}) of 312,47 m^2/g. Structural and morphological characterizations using XRD and SEM confirmed the strong attachment of Fe_3O_4 nanoparticles onto the surfaces of GO and AC, forming a stable AC/GO/Fe_3O_4 composite.

The Cr (VI) adsorption performance of the material was evaluated, achieving a removal efficiency of approximately 97% under the conditions of pH = 2, an initial Cr (VI) concentration of 3 mg/L, an adsorbent dosage of 0,04 g, and an adsorption time of 90 minutes. Adsorption kinetics followed a pseudo-second-order model, while equilibrium data fitted well with the Langmuir isotherm, indicating monolayer adsorption governed by both physical and chemical interactions. Compared to pure AC, AC/GO/Fe_3O_4 exhibited superior adsorption capacity under identical conditions and maintained over 80% efficiency after five adsorption–desorption cycles.

With high adsorption performance, good reusability, and the utilization of agricultural waste (sugarcane bagasse) as a precursor, AC/GO/Fe_3O_4 is considered a promising material with high commercialization potential for heavy metal-contaminated water treatment.

References

1. Solomon Tibebu, Estifanos Kassahun, Tigabu Haddis Ale, Abebe Worku. (2024). The application of Rumex Abysinicus derived activated carbon/bentonite clay/graphene oxide/iron oxide nanocompositefor removal of chromiumfrom aqueous solution. *Scientific reports*.
2. Thi Hong Nhung Nguyen, Duc Dung Mai Anh Son Hoang, Sy Hieu Pham, Thi Lan Nguyen. (2024). Preparation of Fe3O4/graphene oxide nanocomposites on activated carbon for As(V) removal from aqueous solutions. *Journal of Porous Materials* .
3. Hailu Ashebir, Solomon Tibebu, Dinaol Bedada. (2024). Advanced methylene blue adsorption with a tailored biochar/graphene oxide/magnetite nanocomposite: characterization, optimization, and reusability. *Biomass Conversion and Biorefiery* .
4. Lalise Wakshum, Kenatu Angassa, Jemal Fito, Hailu Ashebir&Seble. (2024). Investigation of magnetite graphene oxide- impregnated activated carbon of Rumex abyssinicus stem for adsorption of Cr (VI) from tannery wastewater. *Biomass Conversion and Biorefinery*.